# The Evaluation of Entropy-based Algorithm Towards the Production of Closed-Loop Edge

Cahyo Crysdian [a,*]

[a] *Computer Science Department, Universitas Islam Negeri Maulana Malik Ibrahim Malang, Lowokwaru, Malang, Indonesia*
*Corresponding author: [*]cahyo@ti.uin-malang.ac.id*

*Abstract*— **This research concerns the common problem of edge detection that produces a disjointed and incomplete edge, leading to the misdetection of visual objects. The entropy-based algorithm can potentially solve this problem by classifying the pixel belonging to which objects in an image. Hence, the paper aims to evaluate the performance of entropy-based algorithm to produce the closed-loop edge representing the formation of object boundary. The research utilizes the concept of Entropy to sense the uncertainty of pixel membership to the existing objects to classify pixels as the edge or object. Six entropy-based algorithms are evaluated, i.e., the optimum Entropy based on Shannon formula, the optimum of relative-entropy based on Kullback-Leibler divergence, the maximum of optimum entropy neighbor, the minimum of optimum relative-entropy neighbor, the thinning of optimum entropy neighbor, and the thinning of optimum relative-entropy neighbor. The experiment is held to compare the developed algorithms against Canny as a benchmark by employing five performance parameters, i.e., the average number of detected objects, the average number of detected edge pixels, the average size of detected objects, the ratio of the number of edge pixel per object, and the average of ten biggest sizes. The experiment shows that the entropy-based algorithms significantly improve the production of closed-loop edges, and the optimum of relative-entropy neighbor based on Kullback-Leibler divergence becomes the most desired approach among others due to the production of more considerable closed-loop edge in the average. This finding suggests that the entropy-based algorithm is the best choice for edge-based segmentation. The effectiveness of Entropy in the segmentation task is addressed for further research.**

*Keywords*— **Entropy; relative-entropy; edge detection; optimal edge; closed-loop edge; edge detector evaluation.**

## I. INTRODUCTION

The canny operator has widely been admitted being the most powerful and popular method for edge detection [1], [2]. Despite its recognizable performance, Lelore and Bouchara [3] note that the Canny operator tends to produce disjointed contours. This problem is also suffered by almost all edge detector algorithms that range from the classical technique [4], the optimized approach [2], [5]–[9], to even the advanced methods [10]–[14]. It causes difficulty in automatically recognizing and analyzing the content of digital images, as demonstrated by Figure 1. Here, the Canny edge detector is applied to the input image in Figure 1a, which produces the edge map in Figure 1b. Then, an automatic edge-based segmentation is applied to the edge map in Figure 1b to extract the shape of objects. The result is poor image content, as shown in Figure 1f. The open-loop edges caused that to exist in the edge map. Even after tuning the algorithm with various threshold parameters, as shown in Figure 1c-e, it is

still difficult to generate the edge as a closed-loop boundary of the objects, as shown in Figure 1c-e, respectively. Hence, the edge-based segmentation produces many missing objects, as shown in Figure 1g-i, although the objects are tangible to human subjects, as shown in Figure 1a. A similar approach to optimize edge detection by threshold parameter selection had actually been afforded by some researchers that produced insignificant results [10]. Therefore, it is essential to define an optimal edge as a closed-loop boundary of the object that needs to be achieved by every edge detector. Unlike edge detection algorithms, normal human vision is superior to achieving the optimal edge from every object, even in varied and complicated scenes. Of course, it is essential not to confuse the concept of edge as a boundary of the object with the concept of ridge as a raised line on a flat surface.

Meanwhile, the concept of entropy to measure the uncertainty of an event has the potential to facilitate a complete detection of edge and, therefore, solve the above problem. Date back to the work of Shiozaki [15] that

introduced the entropy operator to detect the edge from a digital image, and later was followed by Barba et al. [16] to employ the entropy measurement in a set of cytological images, the result was promising even though it was hard to mention that the product was an edge since what they produced was merely the entropy measures from the content of a digital image. Varied approaches based on Entropy were introduced afterward, such as Hrzic et al. [17] to threshold the product of local Entropy with the standard deviation of pixel distribution in a windowing scheme, Sert and Derya [18] to employ maximum norm entropy, and Aroza et al. [19] to develop cluster entropy as edge detector.

However, less attention has been paid to achieving the optimal edge defined as a complete closed-loop boundary of the object. Hence, it is necessary to extend the progress made by the edge detection community, particularly to deliver a complete closed-loop edge as the product of edge detection to retrieve the image's content completely. This research aims to deliver the extended progress of entropy-based algorithms to achieve the closed-loop edge by evaluating the performance of the entropy-based edge detection family and their enhancement in retrieving the object boundary represented by the optimal edge as defined above.
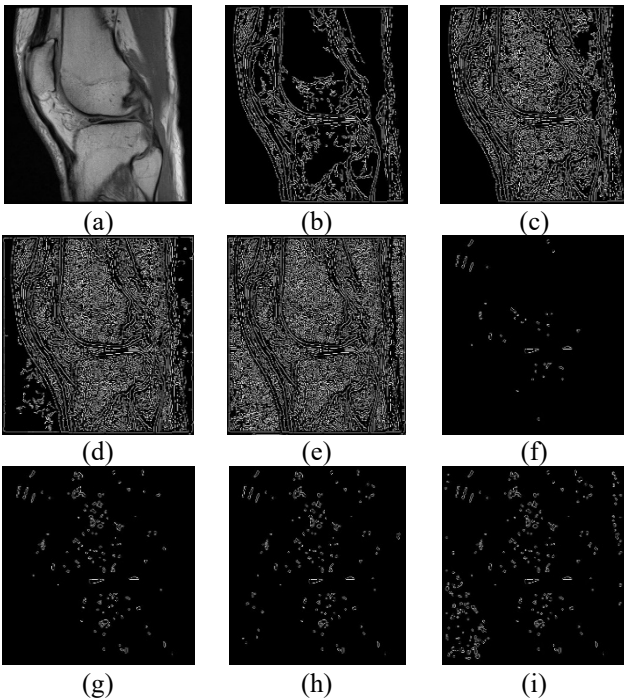


Fig. 1 Edge map generated by Canny for various threshold setting: (a) input image, (b) T1=0.05 & T2=0.125, (c) T1=0.01 & T2=0.05, (d) T1=0.01 & T2=0.02, (e) T1=0.001 & T2=0.002, (f) (g) (h) and (i) the closed-loop edge obtained from b, c, d, and e respectively.

The rest of this paper is organized as follows. Section 2 discusses the approach to optimizing the entropy operator for edge detection rooted in the information-theoretic entropy and the relative entropy. The enhancement of each operator by employing the maximization and minimization approach and further enhancement by applying the thinning algorithm to the entropy map, are presented in this section. Section 3 presents the experiment to measure each algorithm's performance by comparing it against the benchmark of edge detection based on a set of predefined experimental parameters. The analysis

of experimental results is presented in this section. The work is concluded in Section 4.

## II. MATERIALS AND METHODS

### A. The entropy-based edge detector

The concept of Entropy [20], also known as information theoretic entropy [21], is the measurement of system uncertainty that is computed by

$$H = -\sum p_i \ln p_i \tag{1}$$

where $p_i$ is the probability of $i$-th energy state of the system. Equation 1 produces a concave function such as shown by Figure 2, in which the following condition achieves the peak of the function.
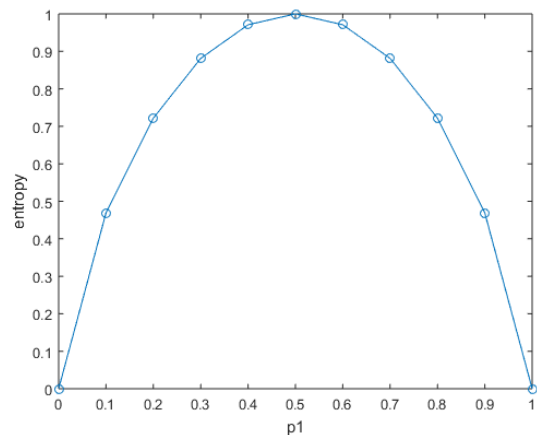
$$p_1 = p_2 = \cdots = p_N \tag{2}$$



Fig. 2 Entropy as a concave function

Equation 2 describes the achievement of maximum uncertainty of an event when it is viewed from the probability of its constituent components. In this case, the condition fulfilled by Equation 2 presents a transition state from an event to other that is acknowledged by a transient point where the uncertainty is maximum. This concept is perfectly matched to edge detection in image analysis. Here, the existence of edge is acknowledged from the transition of pixel membership to an object. For the case that more than an objects exists, the pixel membership of an object gradually changes from high to low, as indicated by the entropy measure.

In this case, the existence of an edge is considered an event influenced by the uncertainty of pixel membership to the existing objects. The edge pixel exists when the pixel membership changes between objects, or where maximum uncertainty tends to take place. Hence, the algorithm needs to facilitate the achievement of maximum uncertainty. Here, we argue that minimizing the number of events tends to achieve maximum uncertainty. Considering the condition where a set of events $A_1 \cdots A_N$ with the corresponding probability $p_1 \cdots p_N$ in which $\sum p_i = 1$, the maximum uncertainty is achieved by fulfilling Equation 2. Here, the maximum uncertainty is a condition among other possible alternatives listed as follows $\{p_1 > p_2 > \cdots > p_N, p_1 > p_2 > \cdots > p_{N-1} = p_N, \cdots, p_1 > p_2 > \cdots > p_{N-1} = p_N\}$. The total number of possible alternatives is

$$\sum A = (N-1)N! + 1 \qquad (3)$$

Hence, the probability to obtain the maximum uncertainty of event A in Equation 3 is described by

$$p_A = \frac{1}{(N-1)N!+1} \qquad (4)$$

Based on Equation 4, minimizing $N$ becomes the only solution to improve the probability of obtaining maximum uncertainty of event $A$. Therefore, it suggests focusing on optimizing the Entropy by computing the number of classes that represent the objects composing an image. This computation influences the sensitivity of Entropy to detect the edge from the pixel structure. In this research, the entropy optimization is computed as follows. For any predefined window $W$ in an image $I$, with $W \subset I$, the Entropy is developed by minimizing the maximum Entropy of $W$, in which the maximum Entropy is obtained by developing $N$ number of classes $c_1 \cdots c_N$ that share equal class probability as defined by Equation. This condition employs the assumption that all pixels are distributed equally to all classes. Hence,

$$c_1 \cdots c_N \subset W \qquad (5)$$

for $N > 1$ with the probability of each class is computed on each window as follows

$$p_i = \frac{|c_i|}{|W|} \qquad (6)$$

Therefore, the Entropy of each window $H$ can be computed by using Equation 1 to develop the entropy map. In this case, $H$ is maximum when Equation 2 is fulfilled, i.e., $p_i = 1/N$ for $i = 1 \cdots N$, hence.

$$H_{MAX} = -\ln\frac{1}{N} \qquad (7)$$

The result in Equation 7 has previously been described by Kapur and Kesavan [21]. Graphing $H$ for $N > 1$ shows the behavior of a concave-like function, as given in Figure 3. Meanwhile, we can rewrite Equation 5 to become $N = f(W, c)$ since $N = |W|/|c|$ for $i = 1 \cdots N$. Since we know that $|W|$ is a predefined constant, here we assume that $|W| = 1$, hence.

$$N = \frac{1}{|c|} \qquad (8)$$

Based on Equation 8, we argue that minimizing the maximum Entropy becomes the foundation to perceive any object's existence in an image.

$$H_{OPT} = \min_i H_{MAX} \qquad (9)$$

By inserting Equation 7 and 8 into Equation 9 to obtain $H_{OPT}$ in terms of $N$ and $c$, we obtain the following results.

$$H_{OPT} \cong \max_i |c| \cong \min_i N \qquad (10)$$

What we find in Equation 10 for $H_{OPT}$ is consistent with Equation 4 and fulfils the graph behavior of $H_{MAX}$ in Figure 3. Therefore, it is necessary to minimize $N$ in order to reach $H_{OPT}$. Solving $N$ for Equation 10 delivers the following solution.

$$N = \begin{cases} 2 & if \quad |W| \in even \\ |W| & if \quad |W| \in prime \\ \min_i \dfrac{|W|}{|c|} & if \quad |W| \in odd \& \neg prime \end{cases} \qquad (11)$$

Proof: For any $|W|$ that is even, $N=2$ become the least divisor to divide $W$ into least number of classes having equal probability, since even number is always completely divided by 2. While for any $|W|$ that is prime, there is no divisor to completely divide prime number except 1 and its own number. However $N=1$ violates Equation 5. Thus, the only solution is $N = |W|$. For any $|W|$ that is odd and not prime, then $|W| = N|c|$. It means $N$ and $|c|$ becomes the factor of $|W|$, therefore solving $N$ needs to simultaneously solving $|c|$. Since we need to minimize $N$ and at the same time maximizing $|c|$ to fulfil Equation 12, it is necessary to have $N \leq |c|$, thus $N = \min_i \frac{|W|}{|c|}$ with $|W|\%|c| = 0$. Therefore, it yields $N \in prime$ since any non-prime number greater than one will always have its factor to violate the minimization principle.
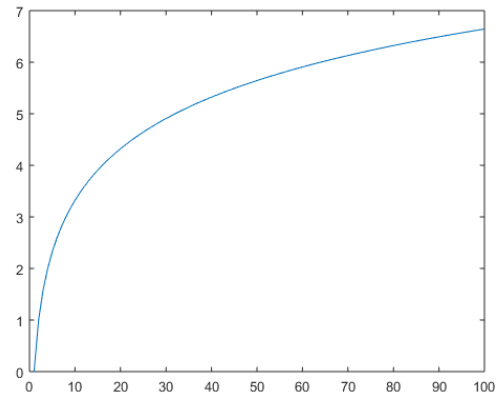


Fig. 3  Behavior of $H_{MAX}$ for $N > 1$

Equation 10 and 11 becomes the foundation of optimum Entropy (OE) to detect the edge of objects in an image. The result of applying OE to image in Figure 1a is given in Figure 4a. Following the definition of edge as the boundary between adjacent objects or between an object and its background, and the importance to achieve the optimal edge as a closed-loop boundary of an object, the application of OE delivers significant advantage to detect and achieve the optimal edge due to twofold. Firstly, the capability of Entropy to measure the uncertainty of a pixel belonging to a certain object based on the condition of its surroundings. Secondly, the condition of the neighboring pixels in an image that generally carry similar values from an object, but experience gradual changes to move between adjacent objects.

In this case, the small changes of pixel values would generate the variation of the Entropy. It is worth noting that higher Entropy leads to the existence of more than an object, and due to OE, the number of available objects have significantly been reduced to a minimum as the target of pixel grouping. Let the entropy map is generated by OE from an image $I$, an edge map $E$ is obtained by optimizing the entropy map based on the maximum of optimum entropy neighbor (MOE) computed by the following equation.

$$E(i,j) = \begin{cases} 1 & if \quad H(i,j) \geq H_{neigh} \\ 0 & if \quad H(i,j) < H_{neigh} \end{cases} \quad (12)$$

Equation 12 shows that the Entropy of each pixel is compared against its neighbors in all directions to identify the existence of edge or non-edge, which is represented by 1 and 0, respectively. The application of MOE in Equation 12 to the entropy map in Figure 4a delivers the result shown in Figure 4b. Some thick edges appear in Figure 4b due to the existence of some groups of maximum Entropy. Therefore, it is necessary to run an edge thinning algorithm to produce the thinning of a maximum of optimum entropy neighbor (TMOE) as the final edge map that contains the closed-loop boundary of objects with a minimum pixel width as shown in Figure 4c.
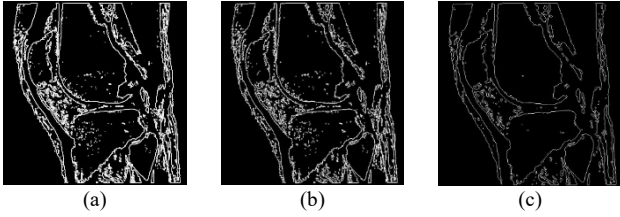


| (a) | (b) | (c) |

Fig. 4 Edge map produced by (a) OE (b) MOE (c) TMOE

B. *The relative-entropy-based edge detector*

A relative entropy [22] is a measure of relative information between two probabilities $p$ and $q$ as computed by

$$H = \sum p_i \ln \frac{p_i}{q_i} \quad (13)$$

Plotting relative Entropy in Equation 13 for $q = 1 - p$ produces a convex function as shown by Figure 5.
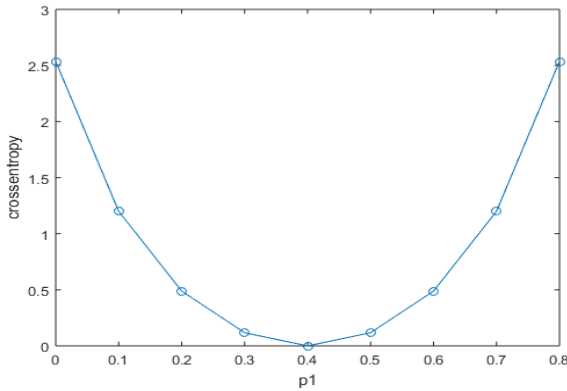


Fig. 5 Relative-entropy as a convex function

It shows that relative Entropy has the opposite behavior to Entropy since it behaves as a convex function as opposed to the Entropy that generates a concave function in Figure 2. Therefore, we need to reverse the operator by minimizing the maximum entropy optimization to obtain the optimum edge detection. The strategy of relative entropy optimization is given as follows.

For any predefined window $W$ in a digital image $I$ with $W \subset I$, the relative entropy optimization is achieved by maximizing the minimum relative Entropy of $W$, in which the minimum relative Entropy is obtained by developing $N$ number of classes $c_1 \cdots c_N$ that share equal class probability

$p_1 \cdots p_N$ given all pixels distributed equally to all classes. Based on Equation 2, $p_i = 1/N$, hence

$$H_{MIN} = \ln \frac{1}{N-1} \quad (14)$$

Proof:

$$\begin{aligned} H_{MIN} &= \min_i \sum_i p_i \ln \frac{p_i}{q_i} \\ &= \sum \frac{1}{N} \ln \frac{1/N}{1-1/N} \\ &= \ln \frac{1}{N-1} \end{aligned}$$

Graphing $H_{MIN}$ in Equation 14 for $N > 1$ delivers a convex-like function as shown by Figure 6.
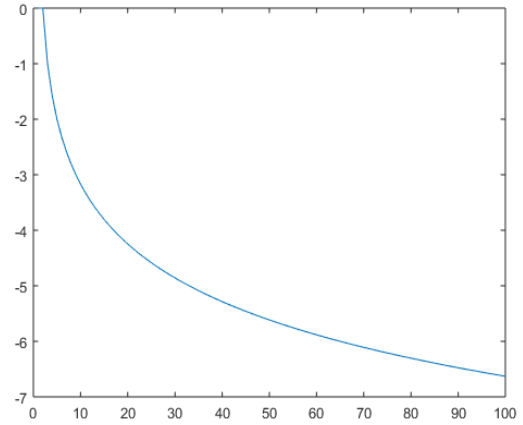


Fig. 6 Behavior of $H_{MIN}$ for $N > 1$

By employing the opposite entropy optimization principle as defined by Equation 9, the optimum of relative Entropy (OR) is computed by maximizing $H_{MIN}$, hence.

$$H_{OPT} \cong \min_i N \quad (15)$$

OR in Equation 15 delivers the same information as OE in Equation 9. Hence, minimizing the number of classes representing the number of objects becomes the foundation of optimizing Entropy and relative Entropy. Since we deal with a convex function as the main characteristic of relative Entropy, we employ the minimum of optimum relative entropy neighbors (MOR) to detect the object edge as given by

$$E(i,j) = \begin{cases} 1 & if \quad H(i,j) \leq H_{neigh} \\ 0 & if \quad H(i,j) > H_{neigh} \end{cases} \quad (16)$$

Applying OR in Equation 15 to an input image in Figure 1a and applying MOR in Equation 16 to the result of OR deliver the results as shown by Figure 7a and 7b, respectively. Figure 7a shows some thick edges due to the gradual changes of relative Entropy from high value to the low value and back to high value again. In this picture, the objects are represented by high value or white color. The application of MOR is able to reduce the thickness of edge as shown by Figure 7b even though it is insignificant to influence the object size. Significant reduction of edge is recorded by inserting the output of MOR in Figure 7b to a thinning algorithm that produces the thinning of maximum relative entropy neighbors

(TMOR), in which the result is shown in Figure 7c. Here, TMOR produces a set of closed-loop edges that have a pixel width.
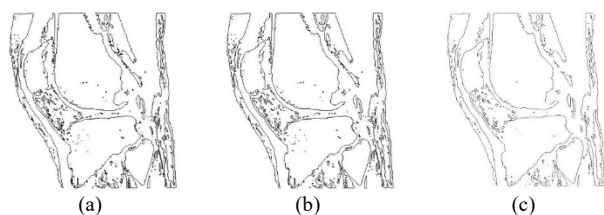


Fig. 7  Edge map produced by (A) OR (B) MOR (C) TMOR

## III. RESULT AND DISCUSSION

The experiment is based on empirical evaluation [23], to measure the performance of entropy-based algorithms to support the automatic segmentation to localize the image content as a set of regions. It utilizes the dataset of knee images obtained from Knoll et al. [24]. The experimental results in segmented regions are derived from the automatic segmentation algorithm [25]–[27] after being supplied by the output of the developed approaches above, i.e., OE, MOE, TMOE, OR, MOR, and TMOR. We also compare the output of the developed algorithms against Canny algorithm as the benchmark of the edge detector. The sample of experimental results is shown in Figure 8.
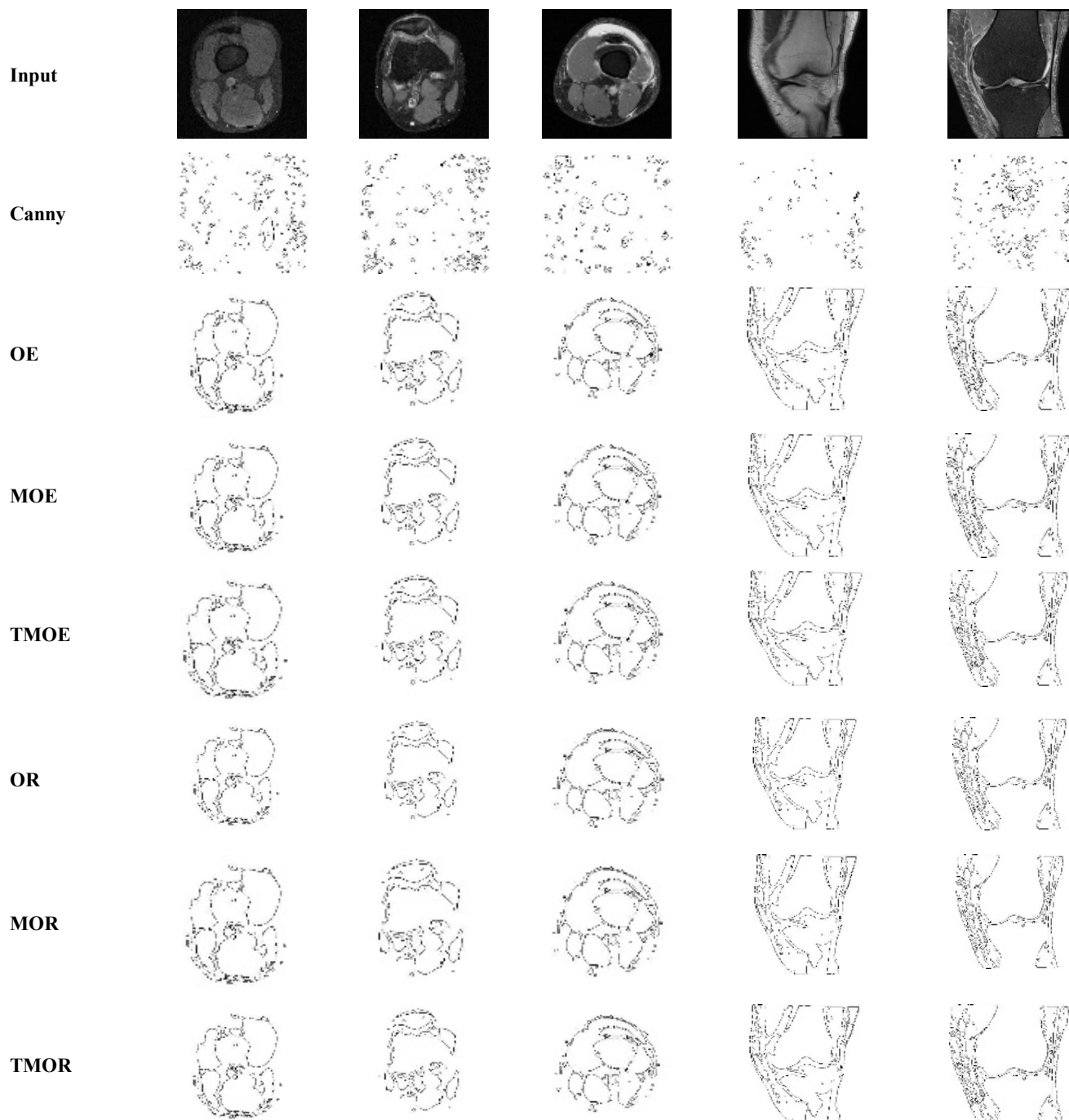


Fig. 8  Sample of experimental results

Rather than employing parameters that appreciate the existence of open-loop edge [28]–[30], the analysis of experimental results is based on set parameters to measure the existence of closed-loop edge, namely the average number of detected objects (s1), the average number of detected edge pixels (s2), the average size of detected objects (s3), the ratio of the number of edge pixel per object (s4), and the average size of tenth biggest objects (s5). These parameters are to identify the requirement to become the desired algorithm, i.e., the method that delivered the meaningful result by producing the significant closed-loop edge while avoiding over-segmentation. The desired algorithm is searched by assigning a rank for each method based on the following sorting mechanism: i.e., minimizing s1 and maximizing s2 - s5. The justification of employing these measurements is as follows. Minimizing s1 refers to the effort to avoid over-segmentation while maximizing s2 - s5 refers to the effort to appreciate the appearance of a significant object that typically occupies a more extensive region and longer edge compared to a meaningless object or noise. The result of measuring s1 – s5 from the edge map produced by each algorithm for 120 test images from Knoll's dataset are shown in Figure 9a–e, respectively.
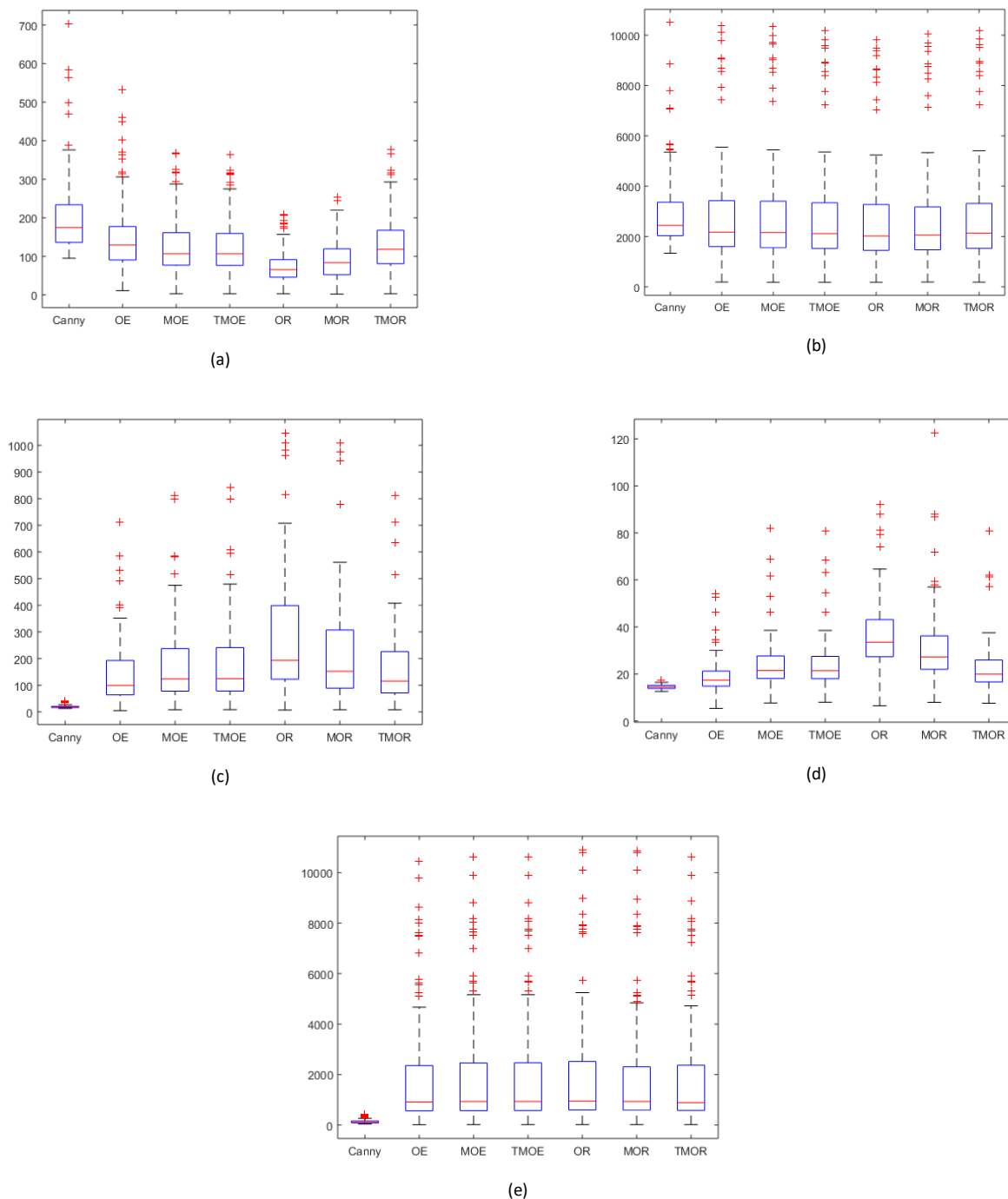


Fig. 9  Experimental results (a) s1; (b) s2; (c) s3; (d) s4; (e) s5

2486

Scrutinizing the experimental result in Figure 9 based on the instrument defined for s1 – s5 delivers the following phenomena. The result of s1 in Figure 9a shows the advantage of the proposed approaches to significantly reduce the number of detected objects even though it does not eliminate over-segmentation. In this case, the OR delivers the highest reduction, which produces a 62.84% reduction compared to Canny, while the lowest is OE, which produces 24.19% reduction. Meanwhile, the result of s2 in Figure 9b presents an insignificant difference in the number of detected edge pixels, although Canny produces a slightly higher number of edge pixels on average compared to the proposed approaches. The results of s3 and s4 in Figures 9c and 9d respectively emphasize the benefits of the proposed approaches to deliver bigger objects and detect more edge pixels per object compared to Canny. Again, OR scores are higher than the other proposed approaches, while OE scores are the lowest. Moreover, the benefit of the proposed approaches is presented by s5 in Figure 9e, in which all proposed approaches significantly score higher than Canny. The experiment proves that the proposed approaches generically improve the production of bigger sizes of closed-loop edges. This finding discloses that the closed-loop network of uncertainty always exists when the Entropy or relative-entropy have enough sensitivity to measure the object's membership from each pixel in an image.

The search for the most desired algorithm is then conducted by assigning the ranking for each detector based on s1 – s5 instrument above, as given by Table 1. The visualization of Table 1 in terms of the rank average and its deviation is given in Figure 10, in which the lowest average of rank score becomes the most desired algorithm. The experimental result shows that the most desired algorithm is held by OR, and then followed by MOE, MOR, and TMOE as the second most desired. The last desired approaches are held by OE, TMOR, and Canny algorithm.

TABLE I
RANK SCORE OF EDGE DETECTOR ALGORITHM

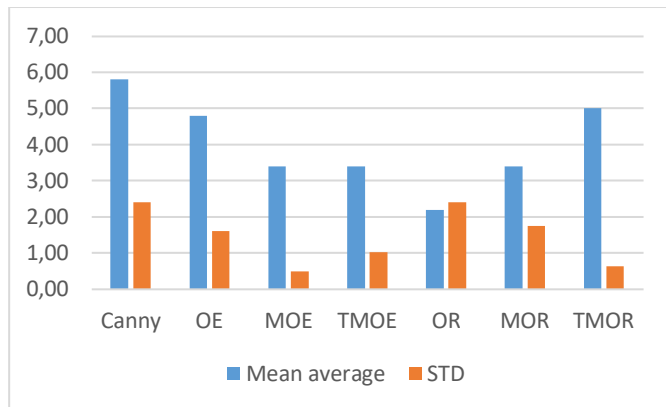| Instrument | Cathe | OE | MOE | TMOE | OR | MOR | TMOR |
|---|---|---|---|---|---|---|---|
| min s1 | 7 | 6 | 4 | 3 | 1 | 2 | 5 |
| max s2 | 1 | 2 | 3 | 5 | 7 | 6 | 4 |
| max s3 | 7 | 6 | 4 | 3 | 1 | 2 | 5 |
| max s4 | 7 | 6 | 3 | 4 | 1 | 2 | 5 |
| max s5 | 7 | 4 | 3 | 2 | 1 | 5 | 6 |



Fig. 10  The ranking of desired methods based on the average rank score. Lowest score become the most desired method.

## IV. CONCLUSION

The mechanism of entropy-based algorithms matches the edge detection task, i.e., to detect an edge point by measuring the uncertainty of pixel membership to the closest object in an image. This approach follows the behavior of an object in a natural scene in which the closer position of a point to the center of the object exhibits higher membership of the point to the object, while the closer position to the edge exhibits lower membership. In this case, the higher membership to an object is represented by the lower entropy value or higher relative entropy. The edge point is acknowledged by detecting the maximum uncertainty that is acknowledged by higher Entropy or lower relative entropy in a neighboring environment.

This approach enables the achievement of a closed-loop edge as long as the Entropy or relative-entropy is sensitive enough to measure the uncertainty of object membership. The benchmark shows that Entropy, relative-entropy, and their enhancements deliver better performance to generate closed-loop edge compared to Canny algorithm. Hence, it is worth noting that the future edge detection algorithm capable of retrieving complete boundary information from the image will soon be dominated by the entropy-based algorithm. The experiment also shows some cases where Entropy or relative-entropy poorly presents the content of an image due to the dominant blurry scene occupying a wide histogram that spans from the dark to bright pixels. In this condition, further optimization of Entropy and relative entropy are required to extend their sensitivity to deal with pixel uncertainty. Further research activities will address this issue.

## CONFLICTS OF INTEREST

The authors declare no conflict of interest.

## REFERENCES

[1] G. Papari and N. Petkov, "Edge and line oriented contour detection: State of the art," Image and Vision Computing, vol. 29, no. 2–3, pp. 79–103, Feb. 2011, doi: 10.1016/j.imavis.2010.08.009.

[2] J. Gimenez, J. Martinez, and A. G. Flesia, "Unsupervised edge map scoring: A statistical complexity approach," Computer Vision and Image Understanding, vol. 122, pp. 131–142, May 2014, doi:10.1016/j.cviu.2014.02.005.

[3] T. Lelore and F. Bouchara, "FAIR: A Fast Algorithm for Document Image Restoration," IEEE Transactions on Pattern Analysis and Machine Intelligence, vol. 35, no. 8, pp. 2039–2048, Aug. 2013, doi:10.1109/tpami.2013.63.

[4] A. K. Bharodiya and A. M. Gonsai, "An improved edge detection algorithm for X-Ray images based on the statistical range," Heliyon, vol. 5, no. 10, p. e02743, Oct. 2019, doi:10.1016/j.heliyon.2019.e02743.

[5] C. Crysdian, "Performance measurement without ground truth to achieve optimal edge," International Journal of Image and Data Fusion, vol. 9, no. 2, pp. 170–193, Oct. 2017, doi:10.1080/19479832.2017.1384764.

[6] M. Mittal et al., "An Efficient Edge Detection Approach to Provide Better Edge Connectivity for Image Analysis," IEEE Access, vol. 7, pp. 33240–33255, 2019, doi: 10.1109/access.2019.2902579.

[7] I. Tabiai et al., "Hybrid image processing approach for autonomous crack area detection and tracking using local digital image correlation results applied to single-fiber interfacial debonding," Engineering

Fracture Mechanics, vol. 216, p. 106485, Jul. 2019, doi:10.1016/j.engfracmech.2019.106485.

[8] O. Li and P.-L. Shui, "Noise-robust color edge detection using anisotropic morphological directional derivative matrix," Signal Processing, vol. 165, pp. 90–103, Dec. 2019, doi:10.1016/j.sigpro.2019.06.036.

[9] V. Roth and T. Vetter, Eds., Pattern Recognition. Springer International Publishing, 2017. doi: 10.1007/978-3-319-66709-6.

[10] W. Yang, W. Wu, X.-D. Chen, X. Tao, and X. Mao, "How to use extra training data for better edge detection?," Applied Intelligence, vol. 53, no. 17, pp. 20499–20513, Apr. 2023, doi: 10.1007/s10489-023-04587-4.

[11] Y. Lu, C. He, Y. Yu, G. Xu, H. Zhu, and L. Deng, "Vector co-occurrence morphological edge detection for colour image," IET Image Processing, vol. 15, no. 13, pp. 3063–3070, Jun. 2021, doi:10.1049/ipr2.12290.

[12] K. Park, M. Chae, and J. H. Cho, "Image Pre-Processing Method of Machine Learning for Edge Detection with Image Signal Processor Enhancement," Micromachines, vol. 12, no. 1, p. 73, Jan. 2021, doi:10.3390/mi12010073.

[13] Y.-J. Cao, C. Lin, and Y.-J. Li, "Learning Crisp Boundaries Using Deep Refinement Network and Adaptive Weighting Loss," IEEE Transactions on Multimedia, vol. 23, pp. 761–771, 2021, doi:10.1109/tmm.2020.2987685.

[14] T. Brosch, J. Peters, A. Groth, T. Stehle, and J. Weese, "Deep Learning-Based Boundary Detection for Model-Based Segmentation with Application to MR Prostate Segmentation," Lecture Notes in Computer Science, pp. 515–522, 2018, doi: 10.1007/978-3-030-00937-3_59.

[15] A. Shiozaki, "Edge extraction using entropy operator," Computer Vision, Graphics, and Image Processing, vol. 36, no. 1, pp. 1–9, Oct. 1986, doi: 10.1016/s0734-189x(86)80025-1.

[16] J. Barba, H. Jeanty, P. Fenster, and J. Gil, "The use of local entropy measures in edge detection for cytological image analysis," Journal of Microscopy, vol. 156, no. 1, pp. 125–134, Oct. 1989, doi:10.1111/j.1365-2818.1989.tb02911.x.

[17] F. Hržić, I. Štajduhar, S. Tschauner, E. Sorantin, and J. Lerga, "Local-Entropy Based Approach for X-Ray Image Segmentation and Fracture Detection," Entropy, vol. 21, no. 4, p. 338, Mar. 2019, doi:10.3390/e21040338.

[18] E. Sert and D. Avci, "A new edge detection approach via neutrosophy based on maximum norm entropy," Expert Systems with Applications, vol. 115, pp. 499–511, Jan. 2019, doi: 10.1016/j.eswa.2018.08.019.

[19] J. Martínez-Aroza, J. F. Gómez-Lopera, D. Blanco-Navarro, and J. Rodríguez-Camacho, "Clustered entropy for edge detection,"

Mathematics and Computers in Simulation, vol. 182, pp. 620–645, Apr. 2021, doi: 10.1016/j.matcom.2020.11.021.

[20] C. E. Shannon, "A Mathematical Theory of Communication," Bell System Technical Journal, vol. 27, no. 3, pp. 379–423, Jul. 1948, doi: 10.1002/j.1538-7305.1948.tb01338.x.

[21] J. N. Kapur and H. K. Kesavan, "Entropy Optimization Principles and Their Applications," Water Science and Technology Library, pp. 3–20, 1992, doi: 10.1007/978-94-011-2430-0_1.

[22] Kullback, S., and R. A. Leibler. "On Information and Sufficiency." The Annals of Mathematical Statistics 22, no. 1 (1951): 79–86. http://www.jstor.org/stable/2236703.

[23] Z. Wang, E. Wang, and Y. Zhu, "Image segmentation evaluation: a survey of methods," Artificial Intelligence Review, vol. 53, no. 8, pp. 5637–5674, Apr. 2020, doi: 10.1007/s10462-020-09830-9.

[24] F. Knoll et al., "fastMRI: A Publicly Available Raw k-Space and DICOM Dataset of Knee Images for Accelerated MR Image Reconstruction Using Machine Learning," Radiology: Artificial Intelligence, vol. 2, no. 1, p. e190007, Jan. 2020, doi:10.1148/ryai.2020190007.

[25] Z. Cai, Y. Liang, and H. Huang, "Unsupervised segmentation evaluation: an edge-based method," Multimedia Tools and Applications, vol. 76, no. 8, pp. 11097–11110, Aug. 2016, doi: 10.1007/s11042-016-3542-8.

[26] S. J. Mousavirad, H. Ebrahimpour-Komleh, and G. Schaefer, "Automatic clustering using a local search-based human mental search algorithm for image segmentation," Applied Soft Computing, vol. 96, p. 106604, Nov. 2020, doi: 10.1016/j.asoc.2020.106604.

[27] A. Pemasiri, K. Nguyen, S. Sridharan, and C. Fookes, "Multi-modal semantic image segmentation," Computer Vision and Image Understanding, vol. 202, p. 103085, Jan. 2021, doi:10.1016/j.cviu.2020.103085.

[28] H. Abdulrahman, B. Magnier, and P. Montesinos, "From contours to ground truth: How to evaluate edge detectors by filtering," 2017. [Online]. Available: https://hal.archives-ouvertes.fr/hal-01940337

[29] B. Magnier, "Edge detection: a review of dissimilarity evaluations and a proposed normalized measure," Multimedia Tools and Applications, vol. 77, no. 8, pp. 9489–9533, Sep. 2017, doi: 10.1007/s11042-017-5127-6.

[30] Nagarjuna College of Engineering and Technology and Institute of Electrical and Electronics Engineers, 2019 Global Conference for Advancement in Technology (GCAT) : Bangalore, India, Oct 18-20, 2019.